

# Numerical Modeling of Underground Contiguous Cross-Cuts Applying Finite Element Method

<sup>1</sup>Oluwaseyi A. O., <sup>2</sup>Oso O. O. And <sup>3</sup>Kutelu B. J.

<sup>1,2,3</sup>Department of Mineral and Petroleum Resources Engineering Technology, Federal Polytechnic, Ado-Ekiti

Date of Submission: 05-09-2024

Date of Acceptance: 15-09-2024

## ABSTRACT

In underground mines, there exists zones of mineral exploitation where diverse drifts are constructed for different purposes. The rock mass in this area is always disturbed by vibrations due to blasting and haulage activities and this is the reason why a more precise method should be explored for the study of such zones. Geomechanical parameters were measured insitu in the field and serpentine and gabbro rock samples were taken to the Geominera laboratory to determine the physical and mechanical properties needed for the modelling of the two contiguous cross cuts. Mohr Coulomb criterion was used to model the elastic part of the rock mass while the Hoek-Brown criterion was for the plastic zone employing finite element programme. The model revealed that the maximum principal stress on the crosscuts was 0.81 MPa and the strength factor, 6. The maximum displacement of 0.88 mm was observed in the roof part of the crosscuts and the deformation ranged from 0.001 to 0.01 m<sup>2</sup>. The zone of destruction was observed in the parts of the ceiling and floor. Since the resistance factor of the rock mass is greater than one, therefore, the rock mass is considered stable and need no support. The wooden support with boards is recommended to prevent the falling of pieces of rocks in the suspicious places of the excavation.

**KEYWORDS:** Contiguous, modeling, Finitelement, Underground

## I. INTRODUCTION

In underground mining, exists zones of mineral exploitation where diverse drifts are located for different purposes and one of them is cross-cut dedicated for drawing minerals from stopes. The rock mass in this area experiences heavy influence of vibration due to blasting and haulage activities. Also, the rock mass that is

formed within 100 m from the surface of the earth crust into the mine, is liable to being weakened by the agent of weathering. Furthermore, the excavations constructed in a very deep level of a mine (about 500 to 800 m) can be affected by high pressure where rock bursting could occur. Employment of high precision method, such as numerical, for the analysis of stress in such situations and to predict the state of stress is highly commendable so as to achieve smooth production operations and safety of the workers.

Initially, the mechanics of construction and simple geometric figures are used as the calculation scheme to solve the problem of pressure in underground mine, where the concept of the equilibrium vault and the principle of sliding prism was adopted. Later, the mechanics of the continuous medium was used to solve the problems and the modeling of the construction processes of the underground works (Shen and Kushwaha, 1998). Then, the analysis of the interaction between the practice and the hypothetical formulations that allow specialists to predict the behavior of an underground work began where, it was necessary to quantify the geomechanical characteristics of the rock mass, for a rational, safe and profitable exploitation (Bieniawski, 1989, 2011; Cartaya, 2001; Cabrera et al., 2012; Cabrera and Samaniego, 2013; Malany and Napier, 2011). The above research were carried out by empirical-analytical method and numerical modeling was not used to describe or evaluate the massifs (Noaet et al., 2017).

Modeling is the process by which a representation or model is created to investigate reality. It constitutes a simplified reproduction of reality that fulfills a heuristic function that allows discovering new relationships and qualities of the object of study and its application is closely related to the need to find a mediated reflection of objective reality. In most cases of practical

problems, it is not possible to find an exact solution to the systems of equations that arise, so numerical calculation is used (Ramírez et al., 1991).

There are two main classes of models possible for numerical calculation in the underground mine: continuous models and discontinuous models. Continuous models consider the rock mass as a continuous medium crossed by discontinuities and solve problems in which the behavior of the rock mass can be modeled by means of the differential equations of the mechanics of continua. This type of models is divided into: differential methods, integral methods and hybrid methods. Within the differential methods, the finite element method and the finite difference method are included and are found in the integral methods: boundary element method, boundary integral method and discontinuous displacement method (Zienkiewicz and Taylor, 2000; Hoek, 2007).

On the other hand, discontinuous models consider the rock mass as a set of individual blocks and are particularly useful for studying cases where the deformation of the rock mass takes place mainly as a consequence of the movement of rock blocks bounded by discontinuities in a stress field. In these models, the equilibrium equation is the equation of motion of a simple unit subjected to forces by its immediate neighbors, and the equations define the acceleration of the particles at each instant and therefore their speed and total displacement (Ramírez, et al., 1991).

### Mathematical basis of the models

The mathematical foundation of the models is developed considering the displacement function, the deformations and stresses of the system.

### Displacement function

By the principle of the displacement formulation, a certain block of the volume (V) of the rock mass is selected in the continuous medium that fulfilled the requirement of the system equilibrium and minimum potential energy. To determine the displacement (u) at any point (i) of the finite element which is approximated as a column vector, equation 1 is used:

$$u \approx \hat{u} = \sum_k N_k a_k = [N_i, N_j, \dots] \begin{Bmatrix} a_i \\ a_j \\ \vdots \end{Bmatrix} = Na \quad (1)$$

Where

N – components that described the position of the nodes

a – number of displacement nodes

### System strains and stresses

Knowing the displacement at each point of the system, the strain at each point can be defined by equation 2 which is the matrix notation.

$$\varepsilon = Su = Ba = \begin{Bmatrix} \varepsilon_x \\ \varepsilon_y \\ \tau_{xy} \end{Bmatrix} = \begin{Bmatrix} \frac{\partial u}{\partial x} \\ \frac{\partial u}{\partial y} \\ \frac{\partial u}{\partial y} + \frac{\partial u}{\partial x} \end{Bmatrix} = \begin{bmatrix} \frac{\partial}{\partial x} & 0 \\ 0, & \frac{\partial}{\partial y} \\ \frac{\partial}{\partial y} & \frac{\partial}{\partial x} \end{bmatrix} \begin{Bmatrix} u \\ v \end{Bmatrix} \quad (2)$$

The equilibrium condition is met when the external (W) and internal (U) works produced by the forces and stresses are equalized during displacement. In this case, the sum of the products of the displacement and the corresponding forces represent the external work done (W), while the sum of the products of the deformations and the corresponding stresses represents the internal work (U).

The minimization of the total potential energy ensures compliance with the equilibrium conditions within the limits established by the displacement configuration. The following equation (3) meets the equilibrium condition:

$$-\delta a^T r = \int_V \delta u^T b dV + \int_A \delta u^T \bar{t} dA - \int_V \delta \varepsilon^T \sigma dV \quad (3)$$

where,

a - border displacement

r - external force acting on the body

b - the distributed mass force

u - displacement of the point inside the body.

$\bar{t}$  - distributed external load which acts on the surface, A, of the boundary contour

$\varepsilon$  - the current deformation of the body

$\sigma$  - the current tension of the body

The terms of equation (6) have the following meanings:

In order to obtain optimal system results, which meets the equilibrium condition, the sum of the potential energy of the external loads (W) and the deformation energy of the system (U) must be stationary and minimum for the variations of the displacements acceptable within the determined configuration of the body. Thus, in the problem of elasticity, the total potential energy is not only stationary, but also minimum, since the finite element method seeks such minimum, provided

that it satisfies a determined configuration of displacement.

$$\delta(W + U) = \delta(\Pi) = 0 \quad (4)$$

$\Pi$  - total potential energy

At greater degrees of freedom, the system will be closer to the exact solution, that which ensures complete equilibrium, as long as the displacements tend, to the limit that is towards the true displacement. If true equilibrium requires complete minimization of the total potential energy ( $\Pi$ ), an approximate finite element solution will always yields an approximate energy ( $\Pi$ ) greater than the correct one (Zienkiewicz and Taylor, 1994):

In addition, it should be noted that the discontinuity of the displacements originates infinite deformations in the separation contours, but in the limit, if the size of the subdivisions is reduced, continuity is restored, the system reaches a state of constant deformation that automatically ensures the continuity of the displacements and that satisfies the constant strain criterion. Thus, the equilibrium of the system is reached and a state of constant stresses. Also, it will be evident that no external work would have been lost through the discontinuities between the elements. The elements that meet these conditions will converge to the exact solution (Shen and Kushwaha, 1998; Zienkiewicz and Taylor, 2000).

### Analysis of elasto-plastic behavior

The analysis of the plastic model is based on the incremental theory where stress and strain are related by means of their component in an incremental or differential way. For the elasto-plastic material, the incremental stress-strain relationships are analyzed assuming failure criteria, creep criteria or the law of hardening. The failure criterion,  $f$ , is in function of stress, strain, and other parameters, such that when  $f < k$ , the rock is elastic and when  $f = k$ , the rock is found plastic state,  $k$  is a rupture constant that depends on the properties of the material. Due to the condition of consistency, the function,  $f$ , cannot be greater than  $k$  and by the rupture criterion ( $f$ ), the rupture surface is determined when the elastic deformation region is found inside the rupture surface and outside of it, is

possible to generate much elastic as plastic deformation.

In plastic rock mass models, the total incremental strain is assumed to be composed of the elastic and plastic increments:

$$d\varepsilon_{ij} = d\varepsilon_{ij}^e + d\varepsilon_{ij}^p \quad (5)$$

The creep law is proposed to determine the direction and relative magnitude of the incremental plastic strain, using the principle of the plastic potential function after reaching the rupture surface. For the elastic-plastic model, the total incremental strain is determined by the elastic component,  $d\varepsilon^e$ , the plastic collapse,  $d\varepsilon^c$ , and the plastic-expansive component,  $d\varepsilon^p$ , and is shown in the following equation (6):

$$d\varepsilon = d\varepsilon^e + d\varepsilon^c + d\varepsilon^p \quad (6)$$

In this study, the expression (6) was evaluated through the generalized Hoek-Brown criterion and with the availability of its incremental constitutive matrix, the finite element program, Phase2V6, 2004 was used to solve the elasto-plastic problem of the models considered.

## II. METHODOLOGY

### Field and Laboratory Measurement

Twenty (20) core samples were obtained from geological survey unit of the 'El Descanso Mine in Santa Clara province, in Cuba and were taken to the laboratory of the same company to carry out the tests whereby the physical and the mechanical properties of the serpentine and gabbro intact rocks were determined. Then, the insitu measurement was carried out at the two contiguous cross cuts at level IV of the Mine, as shown in figure 1.

In situ measurements and observation of the following parameters were taken for Serpentine and Gabbro rock mass: dip and dip direction of the discontinuities, its spacing, roughness and the surface conditions. They were quantified through the chart of Sonmez and Ulisay (2002). Also, the perimeters and the areas of the cross cuts were measured and with the data obtained, the parameters for modeling were calculated and determined.

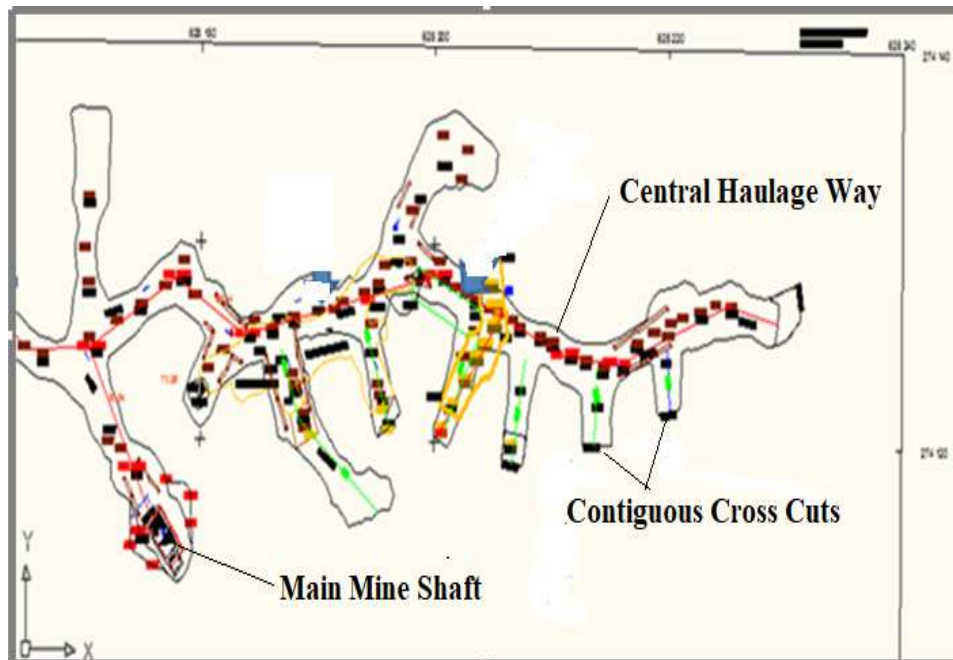


Figure 1, Plan view of the zone of study located at Level IV of 'El Descanso' Underground Mine.

In this research, the finite element method was used due to its ability to calculate and solve problems of complex configurations. It is developed to model the post-rupture behavior of the rock mass, model the interaction between the support and the rock mass, and the homogeneous and non-linear behavior of the rock near the boundaries of the excavation.

The system under study was subdivided into a series of elements of a relatively small size with respect to the system, each of the finite elements has its own equation, so that the equation of the system is obtained by the set of equations of the elements that composed it. Each of these elements has nodes with inherent degrees of freedom. The selection of the size and shape of the element depends on experience, and generally, smaller elements (closer mesh) are designed in the vicinity of the stress concentration zone.

#### Methods of creating models in underground mines

In this study, the stress caused by the gravitational force is insignificant (Hoek and Brown, 1980), therefore, the height of the zone of influence is considered as the height of the load that influences the excavations and by this, the boundary condition is fixed.

#### Formation of the geometry of the models

The parameters selected for modeling is composed of the following models: materials (massive serpentine and gabbro rocks), discontinuities, and two contiguous cross cut and fortification material.

The boundary of the cross cuts was determined and its zone of influence was measured from the center of the excavation, a distance of three times half of its light or diameter, measured towards the inside of the rock mass and the external border of the model is marked. Later, the borders of the materials of the rock mass, the cracks or contacts and the supports were defined.

#### Mesh creation

By establishing the geometry of the area or volume of the block that makes up the model and that satisfies the conditions of minimum potential energy and complete equilibrium of the system, the mesh was created, which divided the domain into finite elements that can be generated in a triangular form. The procedure to create the mesh includes the selection of the type of mesh and its edge is discretized. The mesh is generated by the finite element program and then its quality is checked and if it is correct, the modeling continues and if it is poor, then, it is readjusted. In this investigation, the gradation type mesh was used.

#### Definition of borders and their conditions

A polyline was used to define the boundary of the cross cuts, the rock mass materials and that of the external boundary. The cracks and the support were also defined with the lines. To establish the mode of the models displacement, the boundary conditions was imposed, which can be by segments, nodes or vertices. Also, the field of natural stress states was defined by the following parameters: the major principal stress ( $\sigma_1$ ), the minor principal stress ( $\sigma_3$ ), the stress perpendicular to the plane ( $\sigma_z$ ), the angle between the global coordinate (x) and the direction of the greatest principal stress measured counterclockwise.

### Properties of materials

The materials that were considered for the models under study are: massive serpentine, gabbro, material that constitutes the cracks and the support. Natural in-situ stress properties, material specific weight, elastic properties, plastic properties, stress properties, and discontinuity properties were defined and assigned to these materials. The natural stress state was defined by the gravitational force and the volumetric weight of the rock mass material, which allows the reestablishment of the balance that exists in the stress field before the disturbance caused by the creation of the excavation.

### Stress parameters in the rock mass

For the elasto-plastic analysis of the rock mass; the Mohr-Coulomb criterion ( $c, \Phi$ ) was used to model the strength of the intact rocks which denotes the elastic state of the material, and the parameters of and the constants of the generalized Hoek-Brown criterion ( $m_b, s$  and  $a$ ) that considers the non-linearity of the plastic zone of the rock mass, were defined. This will permit the determination of the degree of destruction of the contour of the excavation. These parameters were determined using the Roclab program (2002) and curves were also obtained that relate the major and minor principal stresses and the brittle or the ductile nature of the rock mass is determined (Mogi, 2007; Oluwaseyi and Ajibola, 2017).

$$T_f = C_i + \sigma_n \tan \phi_i \quad (7)$$

Where,  $T_f$  - shear stress,

$C_i$  and  $\phi_i$  - respectively the cohesion and internal friction angle

$\sigma_n$  - normal stress in the slip plane

$\tan \phi_i$  - the coefficient of internal friction

$$\sigma_1 = \sigma_3 + \sigma_{ci} \left[ m_b \frac{\sigma_3}{\sigma_{ci}} + s \right]^a \quad (8)$$

$$m_b = m_i \exp \left( \frac{GSI-100}{28-14D} \right) \quad (9)$$

$$s = \exp \left( \frac{GSI-100}{9-3D} \right)$$

$$(10)$$

$$a = \frac{1}{2} + \frac{1}{6} (e^{-GSI/15} - e^{-20/3}) \quad (11)$$

$\sigma_1$  and  $\sigma_3$  - effective principal stresses.

$m_b$  - reduced value of Hoek-Brown constant  $m_i$  of the intact rock material.

$\sigma_{ci}$  - linear compressive strength of the intact rock.

$s$  and  $a$  - constants that depend on the characteristics of the studied rock mass.

### The parameters of the discontinuity model

The crack properties that were defined and assigned to the models are: normal stiffness (kn) and shear stiffness (ks). They are determined by the following equations:

$$K_n = \frac{E_i E_m}{L(E_i - E_m)} \quad (12)$$

In the same way, the expression for shear is obtained,  $K_s$

$$K_s = \frac{G_i G_m}{L(G_i - G_m)} \quad (13)$$

$$G_i = \frac{E_i}{2(1+\mu)} \quad (14)$$

$$G_m = \frac{E_m}{2(1+\mu)} \quad (15)$$

Where:

$E_m$  - deformation modulus of the rock mass, which is obtained using the Roclab program (2002).

$G_m$  - shear modulus of the rock mass

$G_i$  - intact rock shear modulus

### Support model parameters

Depending on the type of support, the following properties were determined: Young's modulus (E) and diameter if it is an anchor; and Poisson's ratio ( $\mu$ ) and thickness of shotcrete and were defined and assigned to the support model.

$P_{cr}$  is defined by the expression (16):

$$P_{cr} = \frac{2P_o - \sigma_{cm}}{1+q} \quad (16)$$

$$\sigma_{cm} = \frac{2c \cos \phi}{1 - \sin \phi} \quad (17)$$

$$q = \frac{1 + \sin \phi}{1 - \sin \phi} \quad (18)$$

$$\sigma_1 = \sigma_{cm} + q\sigma_3 \quad (19)$$

Where:

$q$  - the gradient of the graph line  $\sigma_1$  versus  $\sigma_3$



$\sigma_{cm}$ - the uniaxial compressive strength of the rock mass  
 $\sigma_1$ - the axial stress where rupture occurs  
 $\sigma_3$ -the confining stress.  
 $c$ - cohesive stress  
 $\Phi$  – the angle of friction of the rock mass.

The rupture of the rock mass around the excavation occurs when  $P_i < P_{cr}$  and when  $P_i > P_{cr}$  no rupture occurs, and the behavior of the rock mass around it is elastic. The internal radius of elastic displacement,  $\mu_{ie}$  will be:

$$\mu_{ie} = \frac{r_o(1+\mu)}{E} (P_o - P_i) \quad (20)$$

E - Young's Modulus

$\mu$ - Poisson's ratio

At rupture, the plastic radius,  $r_p$  is given by:

$$r_p = \left[ \frac{2(P_o(q-1)+\sigma_{cm})}{(q+1)((q-1)P_i\sigma_{cm})} \right]^{\frac{1}{(q-1)}} \quad (21)$$

And the plastic radial internal displacement of the gallery wall,  $u_{ip}$  will be

$$u_{ip} = \frac{r_o(1+\mu)}{E} \left[ 2(1-\mu)(P_o - P_i) \left( \frac{r_p}{r_o} \right)^2 - (1-2\mu)(P_o - P_i) \right] \quad (22)$$

### Results and Analysis of the Contiguous Crosscuts Model

Table1. Parameters and Physico-mechanical properties of the intact rock, Descanso Mine

Parameters	GSI	$m_i$	D	$\sigma_{ci}$ (MPa)	Young Modulus (MPa)	Coef. of Poisson	CohesiónMPa.	Friction Angle 90 (°)	Volumetric weight
Serpentine	62.5	21	0.7	38.66	1408.29	0.12	6.88	48	2.80
Gabbro	62.5	30	0.7	89.14	2014.84	0.18	18.44	41	3.00

Table 2. Parameters and Physico-mechanicals properties of the rock mass, Descanso Mine

Parameters	$m_b$	s	a	Cohesion, MPa.	Internal friction angle (°)	Volumetric weight (MN/m <sup>3</sup> )	Max principal stress ( $\sigma_{v1}$ ) KPa	Min. principal stress ( $\sigma_{h3}$ ) KPa	Angle between $\sigma_{v1}$ & eje. x	Tensional stress, MPa	Uniaxial Comp. Str, MPa	Global Stress, MPa	Deformation Modulus MPa
Serpentinita masiva	2.7	0.004	0.50	2.250	34.50	0.026	2.5	2.2	60	0.063	2.521	8.55	8299.35
Gabro	3.8	0.004	0.50	5.768	37.59	0.029	2.61	2.2	60	0.102	5.812	23.44	12602.30

Parameters	Critical Stress	Distance between cracks(m)	Normal Stiffness, $K_n$ (MPa/m)	Shear Stiffness, $K_s$ (MPa/m)	Average $K_n$ (MPa/m)	Average $K_s$ (MPa/m)
Serpentine	0.40	0.31	6281.52	2804.24	5696.54	2485.09
Gabbro	3.26	0.31	5111.56	2165.93		

Tabla3. Parameters for modeling outstanding discontinuities at the crosscut zone of the Descanso Mine

Table 4. Values of the properties of the materials for support, Descanso Mine

Parameters	Young Mod. (anchor), MPa	Tensional Capacity (anchor)	Anchor diameter, mm	Young Mod. of shotcrete	Coef. of Poisson, shotcrete	Thickness
Values	20000	0.1MN	25	30000	0.2	0.1

The contiguous cross cuts model (figure 2) is composed of the following components: cross cut 1 and 2, massive serpentine as the main rock mass body, gabbro vein, three prominent cracks, massive serpentine-gabbro contacts, anchors, and shotcrete as support materials. The mesh of the model is of the classified type, it has 950 finite elements and 599 three-node triangular nodes, only three of these finite elements are of poor quality because it has a length ratio greater than 10. The gallery was deformed in  $0.01 \text{ m}^2$ . The properties of the shotcrete are: elastic material with a thickness of 0.1 m, Young's modulus 30,000 MPa and Poisson's ratio, 0.2, and those of the anchors are: diameter, 25 mm, Young's modulus 20,000 MPa and tensile strength 0.1MN. Figures 3 to 6 show the contours and graphs of major principal stress ( $\sigma_1$ ), resistance factor, displacement and strain with graph solution in convergence respectively.

For the model without support (Table 5), the maximum stress are found at the upper right corners and bottom of cross cut 1 and 2, the values are 0.22 MPa and 0.26 MPa respectively, and the minimum of 0.01 MPa, in both crosscuts. The maximum displacement value of crosscut 1 is 0.20

mm and that of 2 is 0.26 mm, both occurred on the ceiling, and the minimum deformation in crosscut 1 is 0.05 mm and that of 2 is 0.09 mm; both occurred in the lower left corner. The maximum value of the resistance factor is 6.00 in the ceiling and floor of crosscut 1 and 2, while in the lower right and upper left corners its minimum value is 1.83. The direction of the deformation runs from the roof downward and the lateral sides move from left to right; Zones of destruction are observed on the ceiling (right part) and the floor (left part) of crosscut 1 and for the crosscut 2, only, on the ceiling (right part).

On the other hand, crosscuts model with anchor support and shotcrete, the following results were observed (Table 5): the maximum stress of 0.77 MPa and 0.81 MPa are recorded at the lower right corners of crosscuts 1 and 2, respectively, and the minimum of 0.04 MPa at crosscut 1. and 0.07 MPa at 2, occurred at the upper and lower right corners of both. the maximum displacement value of crosscut 1 is 0.76 mm and that of 2 is 0.88 mm, both were observed on the roof part, and the minimum of crosscut 1 is 0.28 mm and that of 2 is 0.32 mm, both in the lower left corner; the maximum value of the resistance factor is 6.00, it

occurred at the floor of crosscuts 1 and 2, and its minimum value is 1.30 at the sides. The deformation runs from the roof downward and the sides run from left to right; Zones of destruction was observed at left sides of the ceiling and floor of both crosscuts. Figure 7 shows the main stress interactions of value 1.82MPa in the floors and sides of crosscuts 1 and 2.

The maximum principal stress in crosscuts 1 and 2 with anchor support and shotcrete (0.81 MPa) is higher than that of the crosscuts model without support (0.26 MPa) and it is due to the relative location of the holes and the anchors in the rock mass. Also, the high strength of the serpentine and gabbro rocks together with the healed contacts between them had influenced positively the rock mass strength. Generally, stresses observed, occurred in the section of abrupt change in direction of the excavation contour as can be seen in the analyzed model. According to the research by some authors, it has been proven that sharp sections are always reservoir for stress concentration (Hudson, 2000). Furthermore, the small induced stress produced by the mining activities and the gravity with the inherent internal stress of the rock mass and small rotation between the interfaces of the blocks formed the stress that are concentrated in the corners or vertices of the blocks, developing high local stress and causing a progressive rupture that consequently results in the loss of equilibrium in the rock mass that surround

the excavations. It is also observed that the orientation of the major principal stress exerts a great influence on its contours (figure 3).

The resistance factor which is the ratio between the resistance of the rock and the induced stress is the quantity that measures the level of the rock mass stability. When the induced stress is greater than the resistance of the rock, the rock mass collapses. In the created models, its maximum value is 6, the same for both the one without support and the supported (figure 4). The higher this factor, the better the stability of the rock mass, therefore, it is evident that the model without support is stable and it is not necessary to spend extra support, but the wooden support with boards can be used to prevent the falling of pieces of rocks in the suspicious places. This investigation confirms the mining practice that is ongoing in the zone of the mine under this study.

Also, the maximum displacement of the Crosscuts (1, 2) model without support (0.26 mm) and the one with support (0.88 mm) (figure 5) were observed in the part of the ceiling, the corner and the sides of the model. Although these displacements are small, but their study serves to discover the zone where stress and displacements would occur, so as to proffer adequate solution. Also, the deformations are small, ranging from 0.001 to 0.01 m<sup>2</sup> and are manifested from the roof downward as shown in the model, which is from the left to the right of it (figure 6).

**Table 5. Cross-cuts model results, Descanso mine**

Type of workings	Parameters	Model	
		Crosscut 1	Crosscut 2
Excavation without support	Maximum stress (MPa)	0.22 (DI)	0.26 (DI)
	Minimum stress (MPa)	0,01 (DI)	0,01 (DI)
	Maximum Displacement (mm)	0.20 (T)	0.26 (TLI)
	Minimum Displacement (mm)	0.05 ( II)	0.09 ( II)
	Factor of Resistance maximum	6.00 (T y P)	6.00 (T y P)
	Factor of Resistance minimum	1.83 (DI, IS)	1.83 (DI)
	Deformation (m <sup>2</sup> )	0.01 (THA y LIHD)	0.01 (THA y LIHD)
	Destroyed Zones	TLD y PLI	TLD
	Maximum stress in 3D (in the zone far from the excavation facet, MPa)	4.425	...
	Maximum stress (in the zone close to the excavation face, MPa)	...	...
	Maximum stress (at the excavation face, MPa)		
	Maximum displacement, very far to the face, mm)	8.713	...
	Maximum displacement, close to the face, mm)	...	...



		Maximum displacement, at the face, mm)	...	...
<b>Excavation support with</b>		Maximum stress (MPa)	0.77 (DI)	0.81 (DI)
		Minimum stress (MPa)	0.04 (DS,DI)	0.07 (DS, II)
		Maximum displacement (mm)	0.76 (T)	0.88 (T)
		Minimum displacement	0.28 (II)	0.32 (II)
		Factor of Resistance maximum	6.00 (P)	6.00 (P)
		Factor of Resistance minimum	1.30 (L)	1.30 (L)
		Deformation	THA y	THA y
			LIHD	LIHD
		Destroyed Zone	T y PLI	T y PLI

NOTE: DI – lower right corner; DS – top right corner; LD – right side; T – roof; P – floor; L – side; TLI – left side roof; LI – left side; IS – top left corner; II – lower left corner; TLDS – roof, upper

right side; THA – roof down; LHAd – sides in; LIHD – left side to right; TD – roof to the right; PLI – floor on the left side; TLD – roof on the right side

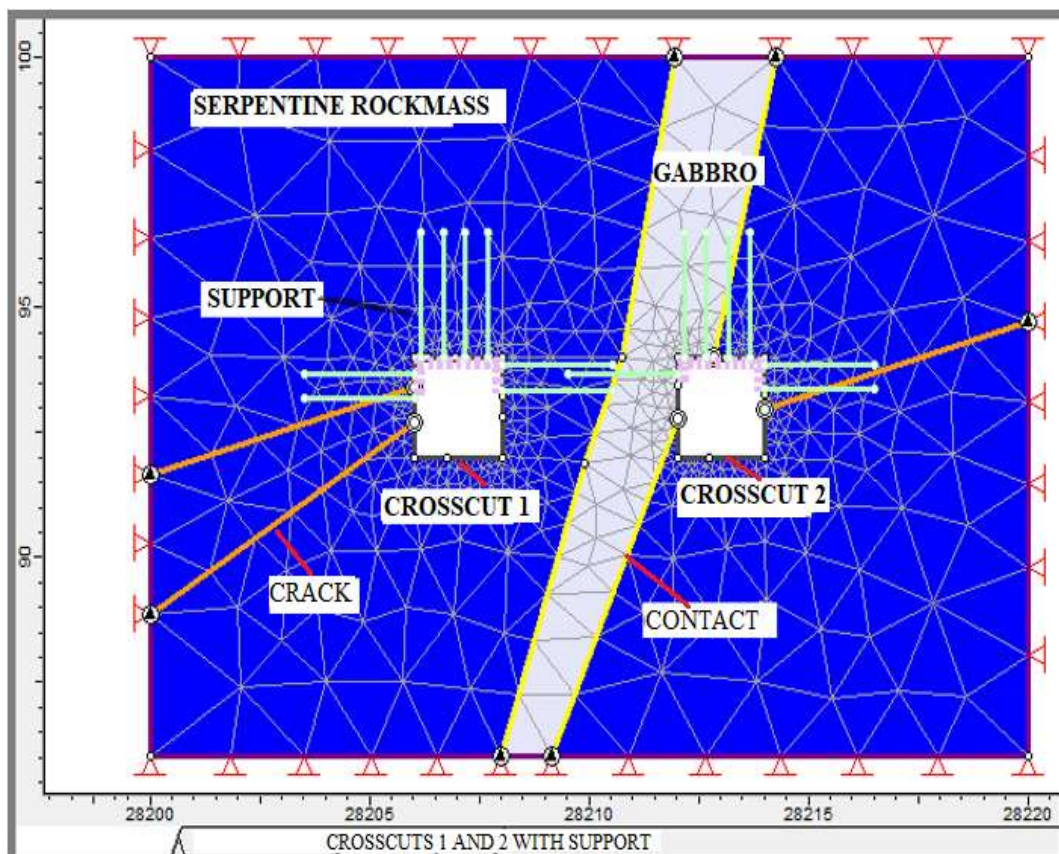


Figure 2. Crosscut Model Mesh, Descanso mine

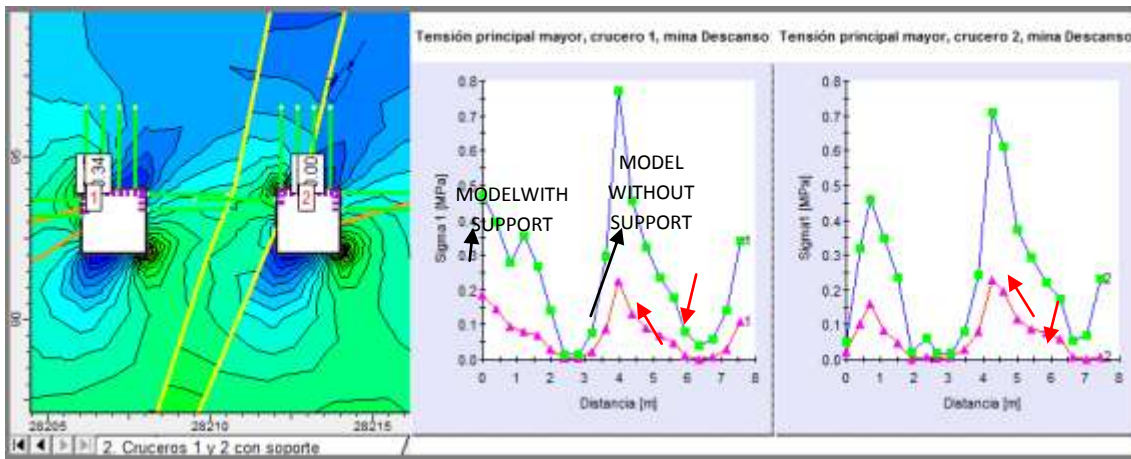


Figure 3. Contour and graph of the major principal stress ( $\sigma_1$ ) of crosscuts model

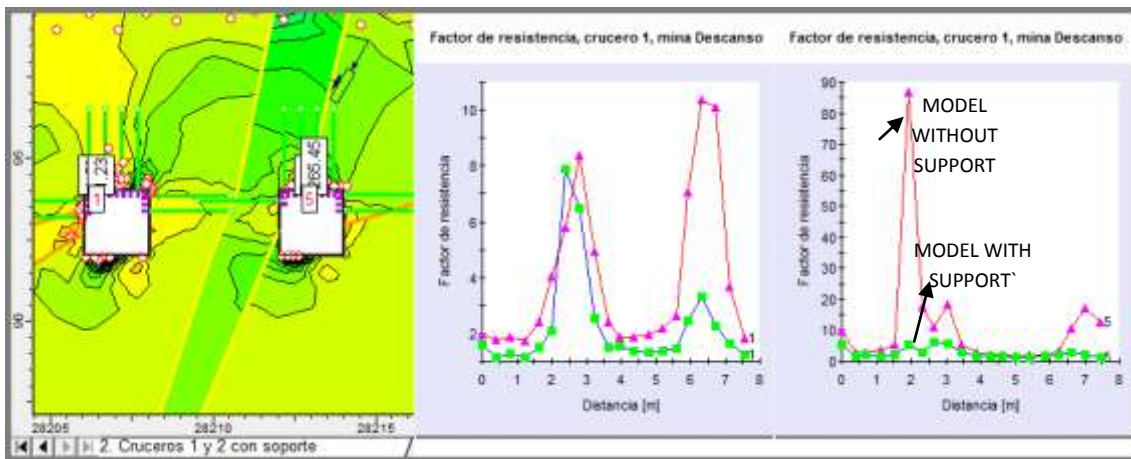


Figure 4. Contour and graph of the resistance factor of crosscuts model

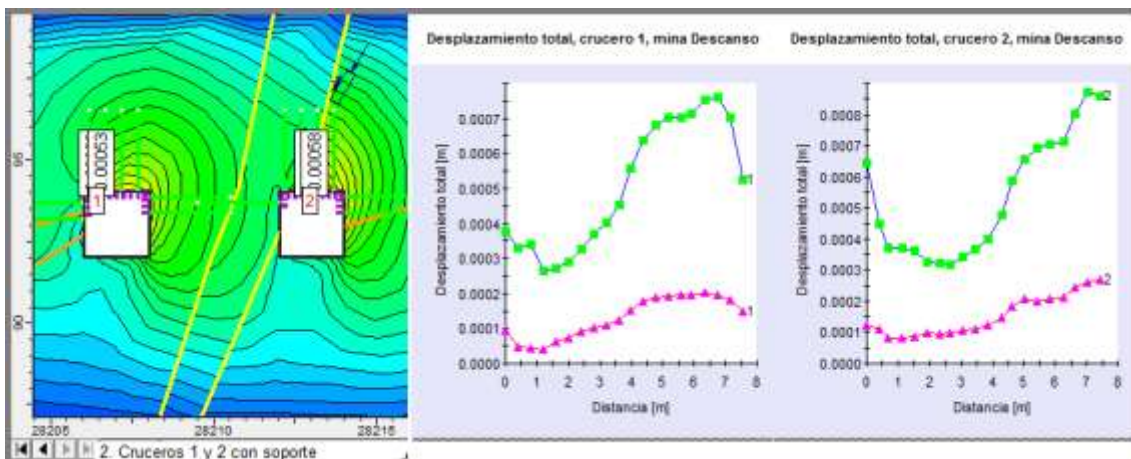


Figure 5. Contour and Displacement Graph of crosscuts Model



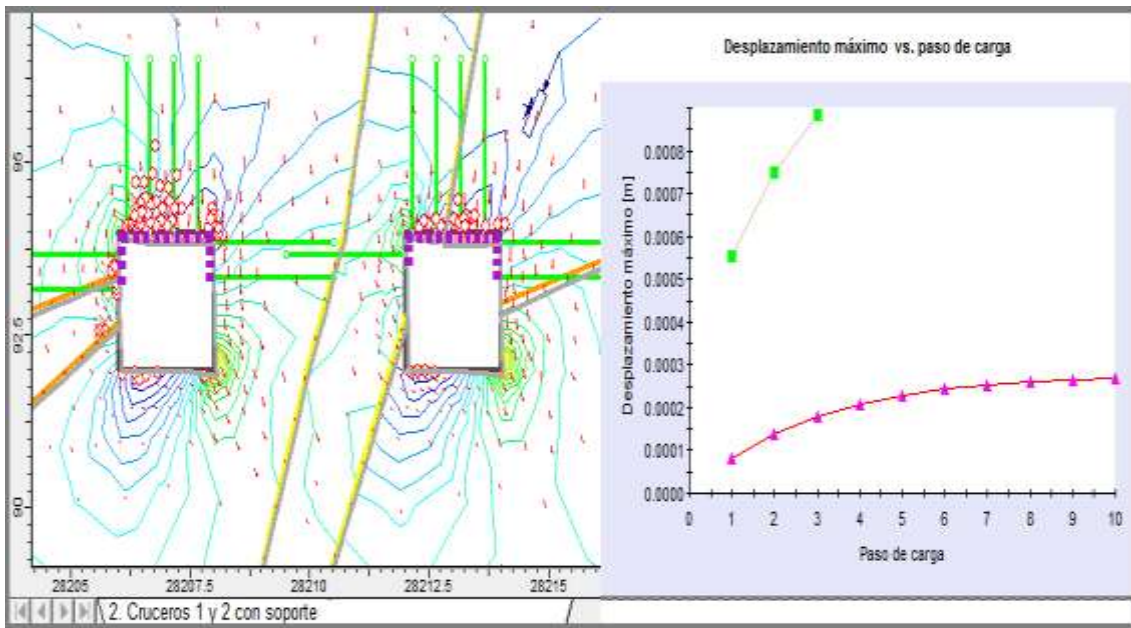


Figure 6. Deformation contour and convergence graph crosscut model

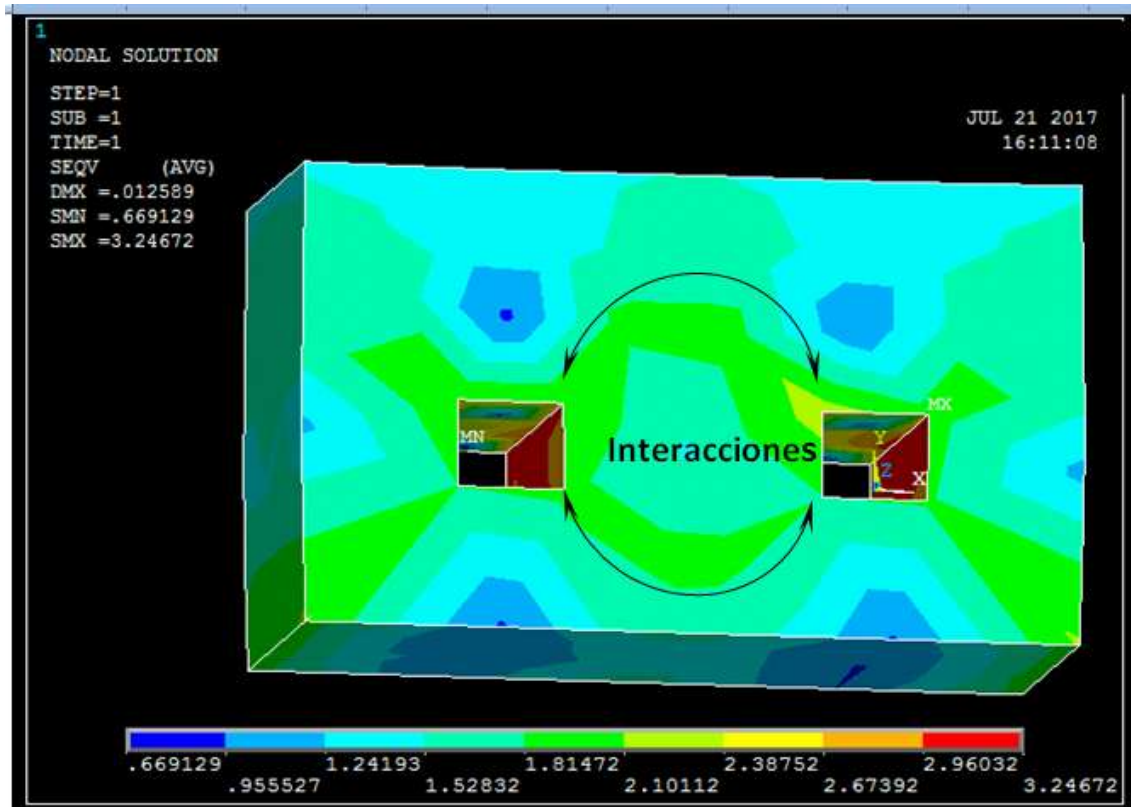


Figure 7. 3D contour of the interactions between cross-cut 1 and 2 model, Descanso mine

The major zone of destruction is observed in some parts of the ceilings and floors of the

contiguous crosscuts model (figure7) which is due to their sharp squared shaped nature. Figure 8

shows that there are stress interactions of value 2.10 MPa between cross-cut 1 and 2, at the top and side part of the model. Small deformation of the contour was also observed (figure 7). It should be noted that the 3D model show higher stress and displacement results than the 2D ones, this is because the influence of prominent discontinuities and the effect of friction on the solid were not considered, and it is assumed that the direction of major principal stresses is vertical.

### III. CONCLUSIONS

The investigation carried out on the two contiguous crosscuts at the level IV of 'El Descanso' Underground mine shows the following conclusions:

- i. The maximum principal stress in crosscuts 1 and 2 with anchor support and shotcrete of 0.81 MPa is higher than that of the crosscuts model without support (0.26 MPa).
- ii. the maximum displacement of the Crosscuts (1, 2) model without support (0.26 mm) and the one with support (0.88 mm) were observed in the part of the ceiling, the corner and the sides of the model and the deformation range from 0.001 to 0.01 m<sup>2</sup> and are manifested from the roof downward
- iii. The major zone of destruction is observed in some parts of the ceilings and floors of the contiguous crosscuts model.
- iv. The resistance factor of the model is greater than one, which means that the strength of the rock mass is greater than the induced stress in the study areas, both for the model without support and as for the one that has support. Therefore, the rock mass is considered stable and need no support.

### REFERENCES

- [1]. Bieniawski, Z.T. 1989: "Engineering Rock Mass Classifications: A Complete Manual for Engineers and Geologists in Mining, Civil and Petroleum Engineering". J. Wiley.
- [2]. Bieniawski, Z. T. 2011: Errores en la Aplicación de las Clasificaciones Geomecánicas y su Corrección. Caracterización Geotécnica del Terreno. Geocontrol Madrid. Pp 2– 30.
- [3]. Cabrera Roberto; Samaniego Antonio & Aduvire Osvaldo 2012: Geomecánica Aplicada al Dimensionado del Método de Minado por Sub Level Stopping. En: 5ª Jornada Iberoamericana técnico-científica Red MASyS 2012-1 Ouro Preto – Brasil.
- [4]. Cabrera, L. Roberto & Samaniego Antonio A. 2013: Diseño Geomecánico del Método De Minado Por Sub Level Stopping. Minería, Edición 430.
- [5]. Cartaya, P. M. 2001: Caracterización Geomecánica de Macizos Rocosos en Obras Subterráneas de la Región Oriental del País. Blanco-Torrens Roberto Cipriano (Tutor). Tesis doctoral, Instituto Superior Minero Metalúrgico de Moa, Cuba. 103p.
- [6]. Hoek, E. 2007: Practical rock Engineering. Rock Mass Properties. In-situ and Induced Stresses. Canadá. 237p, [www.rocksience.com](http://www.rocksience.com)
- [7]. Hoek, E., & Brown, E. T. 1980: Excavaciones Subterráneas en Roca. McGraw-Hill de México S.A. de C.V. pp103-439.
- [8]. Malany D.F. & Napier J. A. L. 2011: The Design of Stable Pillars in the Bushveld Complex mines: a problem solved? Journal of the Southern African Institute of Mining and Metallurgy. 111 (12) Johannesburg.
- [9]. Mogi Kiyoo 2007: Experimental Rock Mechanics. Geomechanics Research series 3. Taylor & Francis Group, London, UK. 380p.
- [10]. Noa Monjes Rafael Rolando, Oluwaseyi Adeoluwa Olajesu & Quevedo Sotovongo Gilberto. 2017: Engineering Characterization of the 'Oro Descanso' Underground Mine Rock mass. In: VII Convention of the Earth Sciences: VII Mining Congress (MINERÍA, 2017), Geological Society of Cuba, Palacio de Convenciones, La Habana, Cuba. 3rd to 7th of April.
- [11]. Oluwaseyi Adeoluwa O. & Ajibola Olawale O. 2017: Estimation of Serpentine Rock Mass Strength of Underground Gold Mine Deposit Placetas, Cuba. FUOYE, Journal of Engineering and Technology, Oye-Ekiti, 2(1):89-94.
- [12]. Phase 2 V6, 2004: A two dimensional elasto-plastic finite element program. Rocscience Inc.
- [13]. Ramírez Oyangüren P.; Irizar L. de la Cuadra; Huerta H. Laín & Obeso E. Grijalbo 1991: Rock Mechanics Applied in the Underground Metallic Mine. Institute of Geology and Mining. Spain. pp114 – 196
- [14]. Roclab, 2002: User's Guide. Rock Mass Strength Analysis using the Hoek-Brown Failure Criterion. Rocscience Inc.
- [15]. Shen Jie & Kushwaha Radhey Lal 1998: Soil-Machine Interactions: A

- FiniteElementPerspective, Marcel Dekker, Inc.(editor) USA, p39-73.
- [16]. Sonmez, H. &Ulusay, R. 2002: A DiscussionontheHoek-Brown FailureCriterion and SuggestedModificationtotheCriterionVerifiedbySlopeStability Case Studies. Yerbilimleri (EarthSciences), 26:77-99.
- [17]. Zienkiewicz, O. Z. & Taylor R. L. 1994: El Método de los Elementos Finitos (E. O. I. d. N. Miguel Cervera Ruiz, Trans. M. J. Norte Ed. 4ta ed. Vol. 1): McGraw Hill Book Company.
- [18]. Zienkiewicz O.C. & Taylor R.L. 2000: TheFiniteElementMethod. Volumen 1: TheBasis. 5ed. Butterworth-Heinemann, Jordan Hill, Oxford, 705p.